


Article

A Closed-Form Parametrization and an Alternative Computational Algorithm for Approximating Slices of Minkowski Sums of Ellipsoids in \mathbb{R}^3

Amirreza Fahim Golestaneh 

Affiliation; mpeafg@nus.edu.sg

Abstract: The current work aims to develop an approximation of the slice of Minkowski sum of finite number of ellipsoids, sliced up by an arbitrarily oriented plane in Euclidean space \mathbb{R}^3 that, to the best of the author's knowledge, has not been addressed yet. This approximation of the actual slice is in a closed form of an explicit parametric equation in the case that the slice is not passing through those zones of the Minkowski surface with high curvatures, namely the "corners". At corners with high curvatures an alternative computational algorithm is introduced in which a family of ellipsoidal inner and outer bounds of the Minkowski's sum are used to construct a "narrow strip" for the actual slice of Minkowski sum. This strip can narrow persistently for a few more number of constructing bounds to precisely coincide on the actual slice of Minkowski sum. This algorithm is also applicable to the cases of slice of Minkowski sum of ellipsoids with high aspect ratio. In line with the main goal, some ellipsoidal inner and outer bounds of the Minkowski sum are reviewed, including the so called "Kurzanski's" bounds. Also some ellipsoidal approximations are suggested for the Minkowski sum, which they can be used, as well as the inner and outer bounds, in calculation of the suggested parametric approximation of the slice of Minkowski sum.

Keywords: slice of Minkowski sum; ellipsoids; closed-form parametrization; approximation; computational algorithm; Kurzanski's bounds

1. Introduction

The Minkowski sum is a binary operator between two sets of position vectors in n -dimensional Euclidean space \mathbb{R}^n , which defines a way to add up the two sets and generate a new set of points with a different geometry. This operator is commutative and associative that allows successive implementation of that to the countable (more practically finite) number of the sets. Let $S_1 \subset \mathbb{R}^n$ and $S_2 \subset \mathbb{R}^n$ be two sets of vectors, then the Minkowski sum $S_1 \oplus S_2 \subset \mathbb{R}^n$ is defined by vector addition of every vector $\mathbf{s}_1 \in S_1$ with every vector $\mathbf{s}_2 \in S_2$

$$S_1 \oplus S_2 \doteq \{\mathbf{s}_1 + \mathbf{s}_2 : \forall \mathbf{s}_1 \in S_1, \forall \mathbf{s}_2 \in S_2\}. \quad (1)$$

This is equivalent to define the Minkowski sum $S_1 \oplus S_2$ as the set of all translated copies of set S_2 by every translation vector $\mathbf{s}_1 \in S_1$

$$S_1 \oplus S_2 \doteq \{\mathbf{s}_1 + S_2 : \forall \mathbf{s}_1 \in S_1\}. \quad (2)$$

From the second definition (2), one can easily imagine that the Minkowski sum of a geometrical shape (object) and a point is the translated shape by the position vector of that point and similarly the sum of an object and a curve is that object swept along the curve. The concepts of Minkowski sum and slice of Minkowski sum are widely used in vast areas of engineering such as crystallography [1,2], robot motion planning [3,4], computer-aided design [5] and assembly planning [6]. One can show that the Minkowski sum of two convex sets is a convex set. This fact allows to define the so-called 'configuration space obstacle' in robotic motion planning. Assume a robot that can move in three-dimensional Euclidean space \mathbb{R}^3 , the 'configuration free-space' of the robot is defined as the set of all positions in space that the robot can inhabit. Conversely the 'configuration space obstacle' is described

as the set of all positions in configuration space that the robot can not attain due to collision with existing fixed obstacles. The geometry and position of the configuration space obstacle depend on geometries and positions of both the obstacle and the robot. Let $P \subset \mathbb{R}^3$ be the set of all points of an obstacle and $R \subset \mathbb{R}^3$ represent the set of points that describes a robot, then one can show that the configuration space obstacle is mathematically determined by Minkowski sum $P \oplus (-R)$, where $-R$ is the inverse of the set R with respect to an arbitrarily selected body-fixed reference frame on the robot R . In this computation the coordinates of every point on robot R is measured with respect to the body-fixed reference frame on R , while the coordinates of points on the obstacle P and also the coordinates of the points in the Minkowski sum $P \oplus (-R)$ are measured with respect to the global frame of reference. The configuration of $P \oplus (-R)$ is geometrically determined by locating the boundary of robot R on the boundary of obstacle P and sweeping it along the boundary of P . In other words the configuration space obstacle $P \oplus (-R)$ is described as the locus of the reference point on the robot R , measured in the global frame of reference, when the boundary of robot R is touching the boundary of obstacle P and sweeping along it. This is similar to interpreting the Minkowski sum $P \oplus (-R)$ as a deformed offset of the set P with variable offset distance. This deformed-offset interpretation was creatively used in [7] to suggest a closed-form parametric equation for the Minkowski sum of two ellipsoids. The novelty in that work is to use the fact that the Affine transformation of an ellipsoid is an ellipsoid, possibly with different sizes of semi-axes and orientation and also to use the concept of offset surface of an ellipsoid.

For the rest of this paper let $E_i(A_i, \mu_i) \subset \mathbb{R}^n$ for $i \in \{1, 2, \dots, m\}$ denotes the so-called "solid ellipsoid" as the set of all points $\mathbf{x} + \mu_i \in \mathbb{R}^n$ that satisfy the implicit relation $E_i = \{\mathbf{x} + \mu_i \in \mathbb{R}^n : \mathbf{x}^T A_i^{-2} \mathbf{x} \leq 1\}$. In this notation $\mu_i \in \mathbb{R}^n$ is the center of ellipsoid E_i , and $A_i = R_i \Lambda(\mathbf{a}_i) R_i^T \in \mathbb{S}^+(n, \mathbb{R})$ is a symmetric positive definite $n \times n$ matrix with real entries, which determines the size and orientation of the ellipsoid E_i such that $R_i \in \mathbb{SO}(n)$ is the rotation matrix corresponding to the orientation of that ellipsoid, $\Lambda(\mathbf{a}_i)$ is the $n \times n$ diagonal matrix with entries $a_i^{(j)}$ of the j th semi-axis length of the solid ellipsoid E_i corresponding to the size of that ellipsoid, for $\mathbf{a}_i = [a_i^{(1)}, a_i^{(2)}, \dots, a_i^{(n)}]$. Note here $\mathbb{S}^+(n, \mathbb{R})$ denotes the set of all symmetric positive definite $n \times n$ matrices with real entries and $\mathbb{SO}(n)$ is the special orthogonal group corresponding to \mathbb{R}^n [8–10]. Similarly the "ellipsoid" is defined as the $n - 1$ dimensional surface, which is embedded in \mathbb{R}^n and encloses the solid ellipsoid E_i , that is $\partial E_i(A_i, \mu_i) = \{\mathbf{x} + \mu_i \in \mathbb{R}^n : \mathbf{x}^T A_i^{-2} \mathbf{x} = 1\}$. Note that in the current work both terms "solid ellipsoid" and "ellipsoid" might be used interchangeably, where the precise meaning is clear from the content. Also here, the word "ellipse" is used with its common meaning as an one-dimensional curve, embedded in \mathbb{R}^n for $n \geq 2$, while the word "ellipsoid" is also used to describe the one-dimensional ellipse, in general. Chirikjian et al. [11] reformed the closed-form formula of the Minkowski sum of two ellipsoids in [7] as:

$$\mathbf{x}_{E_1 \oplus E_2}(\phi) = \mu_1 + A_1 \mathbf{u}_1(\phi) + \frac{A_2^2 A_1^{-1} \mathbf{u}_1(\phi)}{\|A_2 A_1^{-1} \mathbf{u}_1(\phi)\|_2}, \quad (3)$$

where $\|\cdot\|_2$ denotes the Euclidean $\mathbb{L}^2(\mathbb{R}^n)$ norm, $\mathbf{x} = A_1 \mathbf{u}_1(\phi) + \mu_1$ explicitly parametrizes the ellipsoid E_1 centered at $\mu_1 \in \mathbb{R}^n$, $\mathbf{u}_1(\phi) \in \mathbb{S}^{n-1} \subset \mathbb{R}^n$ is the unit vector, parametrized by $n - 1$ angles $\phi = [\phi_1, \phi_2, \dots, \phi_{n-1}]$ and \mathbb{S}^{n-1} denotes the unit sphere embedded in \mathbb{R}^n and centered at origin. Note that in Minkowski sum formula (3), the ellipsoid E_2 is centered at the origin $\mu_2 = \mathbf{0}$ so that the Minkowski sum also presents the configuration space obstacle of the two ellipsoids. This has many applications in robot motion planning, where the geometries of the robot and each obstacle are approximated by the enclosing ellipsoids and then the configuration space obstacle is calculated as the Minkowski sum of two ellipsoids, when the robot ellipsoid is measured in the body-fixed frame of reference located on the center of the ellipsoid $\mu = \mathbf{0}$ [3].

Recall that Minkowski sum is a commutative operator such that $E_1 \oplus E_2 = E_2 \oplus E_1$, however the form of the equation in (3) does not imply the symmetry in formulation, such that $\mathbf{x}_{E_1 \oplus E_2}(\phi_o) \neq \mathbf{x}_{E_2 \oplus E_1}(\phi_o)$ for a particular angular parameter ϕ_o . Therefore, Chirikjian et al. [11] also reformulated a symmetric closed-form parametrization of the Minkowski sum that is more consistent with the commutative characteristic of the Minkowski sum operator. The advantage of this symmetric formula compared to the asymmetric (3) is that they could extend it to the Minkowski sum of countably finite number of ellipsoids (also see [12]):

$$\mathbf{x}_{E_1 \oplus E_2 \oplus \dots \oplus E_m}(\phi) = \boldsymbol{\mu} + \sum_{i=1}^m \frac{A_i^2 \mathbf{u}(\phi)}{\|A_i \mathbf{u}(\phi)\|_2}, \quad (4)$$

where $\boldsymbol{\mu} = \boldsymbol{\mu}_1 + \boldsymbol{\mu}_2 + \dots \boldsymbol{\mu}_m$. As expected from the definition of the Minkowski sum in (1) and (2) the Minkowski sum of ellipsoids is not an ellipsoid. This fact is also inferred from (4), where the sum of countably finite number of symmetric positive definite matrices A_i^2 returns a symmetric positive definite matrix, necessary for generating an ellipsoid, however in this case the formula (4) does not parametrize an ellipsoid, since the denominators are variable parametrized positive scalars, $\|A_i \mathbf{u}(\phi)\|_2$, rather than being fixed positive scalars. At the end it is notable that in literature the Minkowski sum of two ellipsoids was also studied numerically [13–15] or by calculus of ellipsoids [16–18].

For the rest of this paper, some ellipsoidal outer and inner bounds of the Minkowski sum are briefly reviewed, including the so called "Kurzanski's" bounds. Also some ellipsoidal approximations are suggested of the Minkowski sum, which they do not necessarily bound the Minkowski sum from neither inside nor outside, however they are used later, as well as the inner and outer bounds, to derive a closed-form parametrization of the slice of Minkowski sum. This symmetric closed form is to approximate the slice of Minkowski sum in the case that the actual slice does not pass through those zones of the Minkowski surface with high curvature, namely the "corner" zones. The results from model are then compared with the actual slice of Minkowski sum for different ellipsoidal approximations and bounds. Finally, an alternative algorithm is introduced in the case that the actual slice passes closely through the corners of the Minkowski surface with high curvature, in which a family of inner and outer bounds are used to construct a "narrow strip" for the slice of Minkowski sum. This strip can narrow persistently for a few more number of constructing bounds to precisely coincide on the actual slice of Minkowski sum. The strip algorithm is also applied in the case of slice of Minkowski sum of ellipsoids with high aspect ratio.

2. Ellipsoidal Bounds and Ellipsoidal Approximations of Minkowski Sum of Ellipsoids

In this section some ellipsoidal inner and outer bounds and ellipsoidal approximations of the Minkowski sum of ellipsoids are discussed. These bounds and approximations are later used in the following section to derive a closed-form equation of the slice of Minkowski sum.

Given countably finite number of ellipsoids $E_i(A_i, \boldsymbol{\mu}_i) \subset \mathbb{R}^n$ centered at the origin $\boldsymbol{\mu}_i = \mathbf{0}$ for $i = 1, 2, \dots, m$, one can show that every solid ellipsoid defined by:

$$A^2 \doteq \sum_{i=1}^m \gamma_i A_i^2, \quad (5)$$

contains the Minkowski sum $E_1 \oplus E_2 \oplus \dots \oplus E_m \subset \mathbb{R}^n$ as an outer bound for $\forall \gamma_i > 0$ such that [16,19,20]

$$\sum_{i=1}^m \frac{1}{\gamma_i} = 1. \quad (6)$$

Other suggestions for possible coefficients γ_i in (5) were introduced in [11]. Considering again those finite number of arbitrary ellipsoids $E_i(A_i, \boldsymbol{\mu}_i) \subset \mathbb{R}^n$ for $i = 1, 2, \dots, m$ Kurzanski et al. [16,21] presented a family of outer ellipsoidal bounds $E_{ko}(A_{ko}(\mathbf{u}), \boldsymbol{\mu}_{ko}) \subset$

\mathbb{R}^n , centered at $\mu_{ko} = \mu_1 + \mu_2 + \dots \mu_m$, where $A_{ko}(\mathbf{u}) \in \mathbb{S}^+(n, \mathbb{R})$ is parametrized by the unit vector $\mathbf{u} \in \mathbb{S}^{n-1} \subset \mathbb{R}^n$. Similarly, but by different parametrization Durieu et al. [19] suggested a family of outer bounds of the Minkowski sum of finite number of ellipsoids. Compatible with (5), in the case of Minkowski sum of two ellipsoids, a family of outer ellipsoidal bounds $E_\beta(A_\beta(\beta), \mu_1 + \mu_2) \subset \mathbb{R}^n$ is parametrized by $\beta > 0$ [16,22,23]

$$A_\beta^2(\beta) = (1 + \beta^{-1})A_1^2 + (1 + \beta)A_2^2, \\ \beta \in \Gamma_\beta = [\lambda_{min}^{1/2}, \lambda_{max}^{1/2}], \quad (7)$$

where $\lambda_{min} > 0$ and $\lambda_{max} < \infty$ are the roots of the equation:

$$\det(A_1^2 - \lambda A_2^2) = 0. \quad (8)$$

Halder [24] showed that in the case of two ellipsoids the parametrized matrix $A_{ko}(\mathbf{u}) \in \mathbb{S}^+(n, \mathbb{R})$ of the Kurzanski's outer bound $E_{ko}(A_{ko}(\mathbf{u}), \mu_{ko}) \subset \mathbb{R}^n$ in [16,21] is transformed into $A_\beta(\beta) \in \mathbb{S}^+(n, \mathbb{R})$ in (7). He also showed that similarly but by a different transformation the corresponding matrix of the outer bound presented in [19] is transformed into $A_\beta(\beta) \in \mathbb{S}^+(n, \mathbb{R})$ in (7).

The Minkowski sum operator preserves the convexity and compactness of its constituent sets such that the Minkowski sum of convex and compact (closed and bounded) sets is convex and compact. This is used to show that there exists a unique minimum volume outer ellipsoid (MVOE) for the Minkowski sum of countably finite number of ellipsoids [20,24,25]. The MVOE is centered at $\mu_{mvoe} = \mu_1 + \mu_2 + \dots \mu_m$, however no general formula exists for the symmetric positive definite matrix corresponding to that. As a computational solution, Halder [24] studied the optimization problem $\min_{\beta \in (0, \infty)} \log[\det(A_\beta^2(\beta))]$ to determine the $\beta > 0$ in (7) corresponding to the MVOE. He suggested an iterative algorithm to compute the optimal β in (7) of a MVOE (see sub-algorithm A5 in appendix A).

Kurzanski et al. [16] also introduced a family of inner ellipsoidal bounds $E_s(A_{[1,2,\dots,k+1]}(S), \mu_s)$ which bounds the Minkowski sum of $k+1$, $k \geq 1$ number of ellipsoids from inside, where $\mu_s = \mu_1 + \mu_2 + \dots + \mu_{k+1}$ and

$$A_{[1,2,\dots,k+1]}^2(S) = S_k^{-1} \left[(S_k A_{[1,2,\dots,k]}^2 S_k)^{1/2} + (S_k A_{k+1}^2 S_k)^{1/2} \right]^2 S_k^{-1}, \\ A_{[1]} \doteq A_1, \quad S \doteq (S_1, S_2, \dots, S_k), \\ \forall S_i \in \mathbb{S}^+(n, \mathbb{R}), \quad i \in \{1, 2, \dots, k\}. \quad (9)$$

It is of great interest that they showed that the Minkowski sum $E_1 \oplus E_2$ could be precisely constructed from intersection of countably infinite number of outer bounds from (7) or similarly by union of countably infinite number of inner bounds from (9), that means:

$$E_1 \oplus E_2 = \bigcap \{ E_\beta(A_\beta(\beta), \mu_1 + \mu_2) : \forall \beta \in \Gamma_\beta \}, \quad (10a)$$

$$E_1 \oplus E_2 = \bigcup \{ E_s(A_s(S), \mu_1 + \mu_2) : \forall S \in \mathbb{S}^+(n, \mathbb{R}) \}. \quad (10b)$$

This fact is the main inspiration behind the idea in this work to construct a narrow strip from the slices of a few number of inner and outer ellipsoidal bounds of the Minkowski sum that encloses the actual slice of the Minkowski sum such that it is also applicable to the cases in which the actual slice passes closely through the corners of the Minkowski surface with high curvatures such as corners of Minkowski surface of ellipsoids with high aspect ratio of semi-axes.

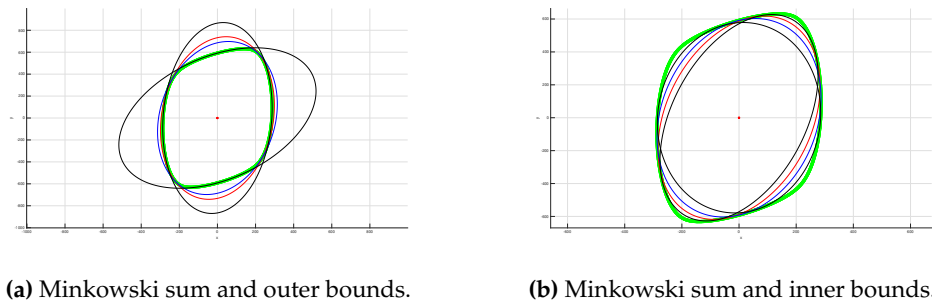


Figure 1. Green: Minkowski sum, Red: Kurzanski's outer for $\beta = 1$ in subplot (a) and Kurzanski's inner for $S_1 = I$ in subplot (b), Blue: MVOE in subplot (a) and John's inner in subplot (b) and Black: Kurzanski's outer for $\beta = \lambda_{\min}^{1/2}, \lambda_{\max}^{1/2}$ in subplot (a) and also Kurzanski's inner for two arbitrary non-identity matrices of $S_1 \in \mathbb{S}^+(n, \mathbb{R})$ in subplot (b).

A so-called "Löwner-John" maximum volume inner ellipsoidal bound of the Minkowski sum of $k+1$, $k \geq 1$ ellipsoids is determined by the symmetric positive definite matrix $C_{k+1}(A_1, A_2, \dots, A_{k+1}) \in \mathbb{S}^+(n, \mathbb{R})$, where [26,27]

$$C_{k+1} = \left[C_k^2 + C_k \left(C_k^{-1} A_{k+1}^2 C_k^{-1} \right)^{1/2} C_k + A_{k+1}^2 + A_{k+1} \left(A_{k+1}^{-1} C_k^2 A_{k+1}^{-1} \right)^{1/2} A_{k+1} \right]^{1/2},$$

$$C_1 \doteq A_1, \quad C_i \doteq C(A_1, A_2, \dots, A_i), \quad i \in \{1, \dots, k+1\}, \quad k \geq 1. \quad (11)$$

This formula is symmetrical in arguments such that $C(A, B) = C(B, A)$. It is notable that the John's (11) and the Kurzanski's (9) formulas return identical inner ellipsoids, that is $A[1, 2, \dots, k+1] = C_{k+1}$, when $S_i \in \mathbb{S}^+(n, \mathbb{R})$ is calculated from:

$$S_i = \left(V \Delta V^T \right)^{1/2} \quad i \in \{1, 2, \dots, k\},$$

$$D = A_{i+1}^{-2} A_{[1, 2, \dots, i]}^2 = V \Lambda V^{-1}, \quad A_{[1]} \doteq A_1, \quad (12)$$

where $V \Lambda V^{-1}$ represents the Eigen-decomposition of the matrix D and Δ is an arbitrary $n \times n$ diagonal matrix with positive entries. This implies that the Kurzanski's inner ellipsoid (9) is independent of choice of diagonal matrix Δ in (12), which is also deducible from (9) as the impact of matrix S_k is cancelled out in the formula.

Fig.1 shows the Minkowski sum of two ellipsoids with outer and inner Kurzanski's bounds. The MVOE and the John's inner bound are also plotted in the sub-figures, successively as the optimal Kurzanski's outer and inner bounds to lay out the outer ellipsoid with the minimum volume and the inner ellipsoid with the maximum volume that bound the Minkowski sum from outside and inside. The Kurzanski's outer bound for $\beta = 1 \in \Gamma_\beta$ in (7) and also the Kurzanski's inner bound for the identity matrix $S_1 = I \in \mathbb{S}^+(n, \mathbb{R})$ in (9) are also plotted for comparison purpose. Fig.1a illustrates that the Kurzanski's outer bounds (7) for minimum and maximum possible values of $\beta = \lambda_{\min}^{1/2}, \lambda_{\max}^{1/2}$ provide maximum coverage of the boundary of Minkowski sum. This observation is in fact in line with the conceptual ideal behind construction of Minkowski sum from the intersection of infinite number of Kurzanski's outers in (10a). Fig.1b displays the Kurzanski's inner bounds for two arbitrary non-identity matrices of $S_1 \in \mathbb{S}^+(n, \mathbb{R})$, which fit into the corners of the Minkowski sum. It is predictable that in general an outer ellipsoidal bound touches a wider region of the Minkowski sum boundary, compared to the touching region between an inner ellipsoid and the Minkowski sum.

Aside from ellipsoidal bounds reviewed above, ellipsoidal approximations of the Minkowski sum are also developed here, which in contrast to the bounds, they neither necessarily enclose the Minkowski sum from outside nor are they fully contained inside the Minkowski sum. However they are used later, as well as the inner and outer bounds, to derive a closed-form model of the slice of Minkowski sum. These ellipsoidal approximations are constructed from replacing the parametrized positive scalar term $\|A_i \mathbf{u}(\phi)\|_2$ for $i \in \{1, \dots, m\}$ in the denominator of the Minkowski formula (4) with some fixed positive scalars $c_i \in \mathbb{R}^+$. As discussed above, this is due to the fact that sum of finite number of symmetric positive definite matrices $\sum_{i=1}^m \frac{A_i^2}{c_i}$, for any positive constant $\forall c_i \in \mathbb{R}^+$ is a symmetric positive definite matrix, which parametrizes an ellipsoidal approximation $\mathbf{x}(\phi) = \sum_{i=1}^m \frac{A_i^2}{c_i} \mathbf{u}(\phi)$ of the corresponding Minkowski sum in (4). Here in \mathbb{R}^3 each denominator in Minkowski sum (4) is replaced by the second eigenvalue $\lambda_2(A_i^T A_i) > 0$ of the matrix $A_i^T A_i \in \mathbb{S}^+(3, \mathbb{R})$ or by the Frobenius norm of the matrix $A_i \in \mathbb{S}^+(3, \mathbb{R})$, so that the explicit parametric relation of the family of ellipsoidal approximations of the Minkowski sum is obtained by:

$$\mathbf{x}(\phi) = \boldsymbol{\mu} + \sum_{i=1}^m \frac{A_i^2 \mathbf{u}(\phi)}{\sqrt{\lambda_2(A_i^T A_i)}}, \quad (13)$$

or by:

$$\mathbf{x}(\phi) = \boldsymbol{\mu} + \sum_{i=1}^m \frac{A_i^2 \mathbf{u}(\phi)}{\|A_i\|_F / \sqrt{n}}, \quad (14)$$

where each ellipsoidal approximation is centered at $\boldsymbol{\mu} = \boldsymbol{\mu}_1 + \boldsymbol{\mu}_2 + \dots + \boldsymbol{\mu}_m$, $n = 3$ denotes the dimension of the space \mathbb{R}^3 and $\|A_i\|_F$ is the Frobenius norm of the matrix $A_i \in \mathbb{S}^+(3, \mathbb{R})$. In this work for any $B \in \mathbb{S}^+(3, \mathbb{R})$ the three positive eigenvalues are assumed to be sorted as $0 < \lambda_1(B) \leq \lambda_2(B) \leq \lambda_3(B)$.

Fig.2 illustrates some ellipsoidal approximations, obtained from (13) and (14), for various geometries of the Minkowski sums of two, three, six and ten number of ellipsoids in \mathbb{R}^2 with different sizes of semi-axes and orientations. As the results show the ellipsoidal approximations do not necessarily bound the Minkowski sum from outside or inside. It is notable that the ellipsoid obtained from Frobenius norm in (14) shows more level of accuracy relative to the actual Minkowski sum. Although these ellipsoids do not approximate the Minkowski sum precisely, they could be used in derivation of the closed-form explicit parametric equation of the slice of Minkowski sum of ellipsoids, as will be discussed in the following section.

3. Slice of Minkowski Sum of Ellipsoids

In this section a closed-form explicit parametric formula is developed to approximate the slice of Minkowski sum of finite number of ellipsoids, sliced up by an arbitrarily oriented plane in Euclidean space \mathbb{R}^3 . This formulation is mathematically of immense interest since the Minkowski sum of ellipsoids is in general a geometry with an irregular shape, which by nature makes its slice ambiguous. Besides that although different closed-form equations of Minkowski sum of ellipsoids were previously developed [7,11], to the best of the author's knowledge a closed-form parametrization of the slice of Minkowski sum of finite number of ellipsoids has not been addressed yet. The main idea behind this derivation is to first approximate the Minkowski sum by an ellipsoid and then slice it up by that plane. The resultant elliptical intersection is then used to define a "spherical sector" of a unit sphere, which is composed of a spherical cap and a cone formed by the center of that unit sphere and the base of that cap (see Fig.3). The base of this cone is a circle, which is mapped to an approximation of the slice of Minkowski sum, by the same transformation (from the parametric equation of Minkowski sum), that maps the unit sphere to the Minkowski sum.

As discussed in previous section, there are several ways to bound (see (5),(7), (9), (11)) or approximate (see (13) and (14)) a Minkowski sum of ellipsoids. Consider an

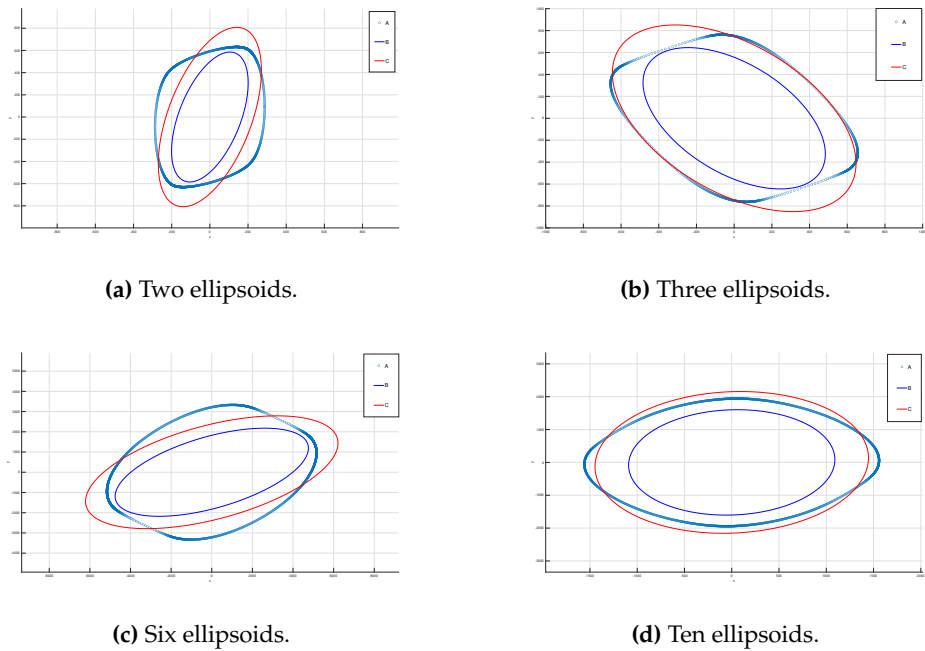


Figure 2. Some ellipsoidal approximations of various Minkowski sums of two, three, six and ten number of ellipsoids. Here curves (A) show actual Minkowski sums. The ellipsoidal approximations are by (B): $(\lambda_2(A_i^T A_i))^{1/2}$ and (C): $\frac{\|A_i\|_F}{\sqrt{2}}$.

ellipsoidal approximation $\partial E(C, \mu) \subset \mathbb{R}^3$ of the boundary of Minkowski sum $\partial(E_1 \oplus E_2 \oplus \dots \oplus E_m) \subset \mathbb{R}^3$ for $i \in \{1, \dots, m\}$, which is centered at $\mu = \mu_1 + \mu_2 + \dots + \mu_m$ and is successively described by the explicit and implicit descriptions $\partial E = \{\mathbf{x}(\phi) = \mu + C\mathbf{u}(\phi)\}$ and $\partial E = \{\mathbf{x} + \mu \in \mathbb{R}^3 : \mathbf{x}^T C^{-2} \mathbf{x} = 1\}$. Recall that $\mathbf{u}(\phi) \in \mathbb{S}^2 \subset \mathbb{R}^3$ is the unit vector, parametrized by two angles $\phi = [\phi_1, \phi_2]$ and \mathbb{S}^2 denotes the unit sphere embedded in \mathbb{R}^3 and centered at origin. Here $C \in \mathbb{S}^+(3, \mathbb{R})$ is a symmetric positive definite matrix, which defines the ellipsoidal approximation of the Minkowski sum and could be obtained from either of (13) or (14) as:

$$C_2 = \sum_{i=1}^m \frac{A_i^2}{\sqrt{\lambda_2(A_i^T A_i)}} \quad (15a)$$

$$C = \sum_{i=1}^m \frac{A_i^2}{\|A_i\|_F / \sqrt{n}} \quad (15b)$$

where $C_2 \in \mathbb{S}^+(3, \mathbb{R})$ in (15a) is the matrix C corresponding to the second eigenvalue $\lambda_2(A_i^T A_i)$.

Let $P \subset \mathbb{R}^3$ be a generally oriented plane embedded in Euclidean space \mathbb{R}^3 , that means $P = \{\mathbf{x} \in \mathbb{R}^3 : \mathbf{n} \cdot \mathbf{x} = h\}$, where \cdot denotes the binary operator of the Euclidean inner product of two vectors, \mathbf{n} is the normal unit vector of the plane and the so-called "height" $h = \mathbf{n} \cdot \mathbf{x}_0$ of the plane is the component of any arbitrary point $\mathbf{x}_0 \in P$ on the plane, along the normal unit vector \mathbf{n} . Now slice up the ellipsoidal approximation ∂E of the Minkowski sum by the plane P , where the elliptical intersection $\partial E \cap P = \{\mathbf{x} \in \partial E : \mathbf{n} \cdot (\mathbf{x} + \mu) = h\}$ is implicitly parametrized by angles $\phi = [\phi_1, \phi_2]$ as $(C^T \mathbf{n})^T \mathbf{u}(\phi) = h - \mathbf{n}^T \mu$, such that from

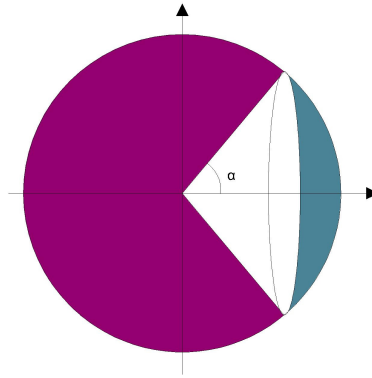


Figure 3. Sphere and cone with its apex on the center of the sphere.

implicit definition of ∂E , $\mathbf{x} = C\mathbf{u}(\phi)$. This implies $\mathbf{c} \cdot \mathbf{u} = \frac{h - \mathbf{n}^T \boldsymbol{\mu}}{\|C^T \mathbf{n}\|_2}$, where the unit vector \mathbf{c} is defined by $\mathbf{c} \doteq \frac{C^T \mathbf{n}}{\|C^T \mathbf{n}\|_2} = [c_1, c_2, c_3]^T$. Since both \mathbf{c} and \mathbf{n} are unit vectors, hence

$$\alpha = \cos^{-1} \left(\frac{h - \mathbf{n}^T \boldsymbol{\mu}}{\|C^T \mathbf{n}\|_2} \right) \quad (16)$$

is used to define a "spherical sector" of a unit sphere. This spherical sector is a portion of the unit sphere composed of a cone with its apex on the center of the sphere and also of a spherical cap (see Fig.3). The base of this cone is a circle, which is explicitly parametrized by

$$\mathbf{u}_c(\phi) = \mathbf{c} \cos(\alpha) + \sin(\alpha) [\mathbf{c}' \cos(\phi) + \mathbf{c}'' \sin(\phi)], \quad (17)$$

where the unit vectors $\mathbf{c}' \doteq \frac{[-c_2, c_1, 0]^T}{\|[-c_2, c_1, 0]^T\|_2}$ and $\mathbf{c}'' \doteq \frac{\mathbf{c} \times \mathbf{c}'}{\|\mathbf{c} \times \mathbf{c}'\|_2}$ and \mathbf{c} are linearly independent, forming an orthonormal basis. Now an approximation of the slice of Minkowski sum is suggested by mapping this circular base of the cone in (17) using the same transformation (from the parametric equation (4) of Minkowski sum), that maps the unit sphere to the Minkowski sum. Therefore, the slice of Minkowski sum of ellipsoids by an arbitrarily oriented plane in \mathbb{R}^3 is explicitly parametrized as a curve embedded in \mathbb{R}^3 by:

$$\mathbf{x}_s(\phi) = \boldsymbol{\mu} + \sum_{i=1}^m \frac{A_i^2 \mathbf{u}_c(\phi)}{\|A_i \mathbf{u}_c(\phi)\|_2}. \quad (18)$$

The planar slice of Minkowski sum is finally obtained from projection of this curve onto the slicing plane P along the normal unit vector \mathbf{n} of the plane. That means the planar slice of Minkowski sum is explicitly parametrized by:

$$\mathbf{x}_p(\phi) = \mathbf{x}_s(\phi) - H(\phi) \mathbf{n}, \quad (19)$$

where $H(\phi) = (\mathbf{x}_s(\phi) - \mathbf{x}_0) \cdot \mathbf{n}$ for any arbitrary point $\mathbf{x}_0 \in P$ on the slicing plane. It is notable that the necessary and sufficient condition under which the arbitrarily oriented plane P slices up the ellipsoidal approximation of the Minkowski sum is:

$$\frac{|h - \mathbf{n}^T \boldsymbol{\mu}|}{\|C^T \mathbf{n}\|_2} \leq 1, \quad (20)$$

which is consistent with (16).

Fig.4 shows a sample of one Minkowski sum of two ellipsoids, sliced up by an arbitrarily oriented plane at different heights of h , for which the actual slice is modeled by the parametric formula in (18) (and its projection onto the slicing plane in (19)), based on

three various ellipsoidal approximations of Minkowski sum. Recall that the formulation of parametric equation (18) of the slice of Minkowski sum is based on calculation of the circular base (17) of a cone, for which an ellipsoidal approximation of the Minkowski sum is required. Among various ellipsoidal outer and inner bounds and also ellipsoidal approximations of the Minkowski sum introduced above, the MVOE from minimization of (7), the John's maximum volume inner bound (11) and the ellipsoidal approximation by matrix C_2 in (15a) from second eigenvalue $\lambda_2(A_i^T A_i)$ for $i \in \{1, 2\}$ are selected here for computation of the parametric slice of Minkowski sum (18). In fact the MVOE and John's maximum volume inner ellipsoid are selected successively as the optimal representatives of the family of parametrized outer Kurzhanski's (7) and inner Kurzhanski's (9) bounds. Recall that here the three positive eigenvalues of any 3×3 symmetric positive definite matrix is assumed to be sorted in ascending order, therefore the ellipsoidal approximations of the Minkowski sum by second eigenvalue is assumed to be a moderate approximation, wisely chosen for computation of parametric slice of Minkowski sum. The Minkowski sum in this sample is constructed from two ellipsoids with aspect ratio of 3, which is the ratio of the length of major axis (longest axis) to the length of minor axis (shortest axis).

Fig.4 illustrates both the parametric slices of Minkowski sum embedded in \mathbb{R}^3 and the corresponding projections onto the slicing plane. Figs.4a and 4b correspond to the case in which the slicing plane is close to the center of the Minkowski sum such that the curve of the actual slice is relatively far enough from the zones of the Minkowski surface with high curvature, namely the "corners" of the Minkowski surface. In such cases, the suggested technique above for modeling the actual slice by (18) and (19), generally provides reliable approximation of the actual slice, such that the accuracy and consistency of the parametric slice with actual one increase, when the actual slice is farther from the "corners" of the Minkowski surface. Precisely, the parametric slice, computed by matrix C_2 in (15a) from second eigenvalue $\lambda_2(A_i^T A_i)$ for $i \in \{1, 2\}$ presents a more consistent approximation with the actual slice of Minkowski sum. In other words, the second eigenvalue-based parametric formula of the slice of Minkowski sum models the actual slice more accurately compared to the Kurzhanski's outer-inner bound-based parametric formulas of the slice.

Figs.4c, 4d, 4e and 4f illustrate identical samples of Minkowski sum to Fig.4a, 4b, sliced up by the same oriented plane, but at larger heights of h for which the parametric slices present weaker approximations. This observation approves the hypothesis that by increasing the distance of the slicing plane from the center of the Minkowski sum toward the "corners" the parametric model will lose the accuracy.

Fig.5 enlightens that the weak consistency of the slice approximations with the actual one, observed in Figs.4c,4d, 4e and 4f is in fact an indirect consequence of distance of the slicing plane (actual slice) from the center of the Minkowski sum. This figure shows a similar slicing sample to Figs.4a,4b such that the same Minkowski sum is sliced up by a plane at the same height h , but with different orientation. Although, the slicing plane is in the same distance h from the Minkowski center as in Figs.4a,4b, the parametric slices show some discrepancy with the actual one at two corners of the projected (planar) slices (see Fig.5b). These corners of the planar slices correspond to slicing of the corners of Minkowski sum with high curvatures (see Fig.5a). In summary, the comparison between Figs.4a,4b and Figs.5a,5b implies that the inconsistency between parametric slice and actual slice of Minkowski sum occurs in the case that the curve of the actual slice passes closely through the corners of the Minkowski surface with high curvature, where the parametric model presents lower accuracy of approximation.

In line with the current discussion on the destructive impact of curvature of the Minkowski surface on the accuracy of the suggested parametric model for the slice of Minkowski sum, Fig.6 represents another type of condition under which the Minkowski surface might likely have high curvature at particular zones. This is the case in which the constituting ellipsoids of the Minkowski sum have "strong" high aspect ratio. For an ellipsoid with a "strong" high aspect ratio, not only the ratio of the lengths of major semi-axis (third semi-axis) to the minor semi-axis (first semi-axis) is high, but also this ratio

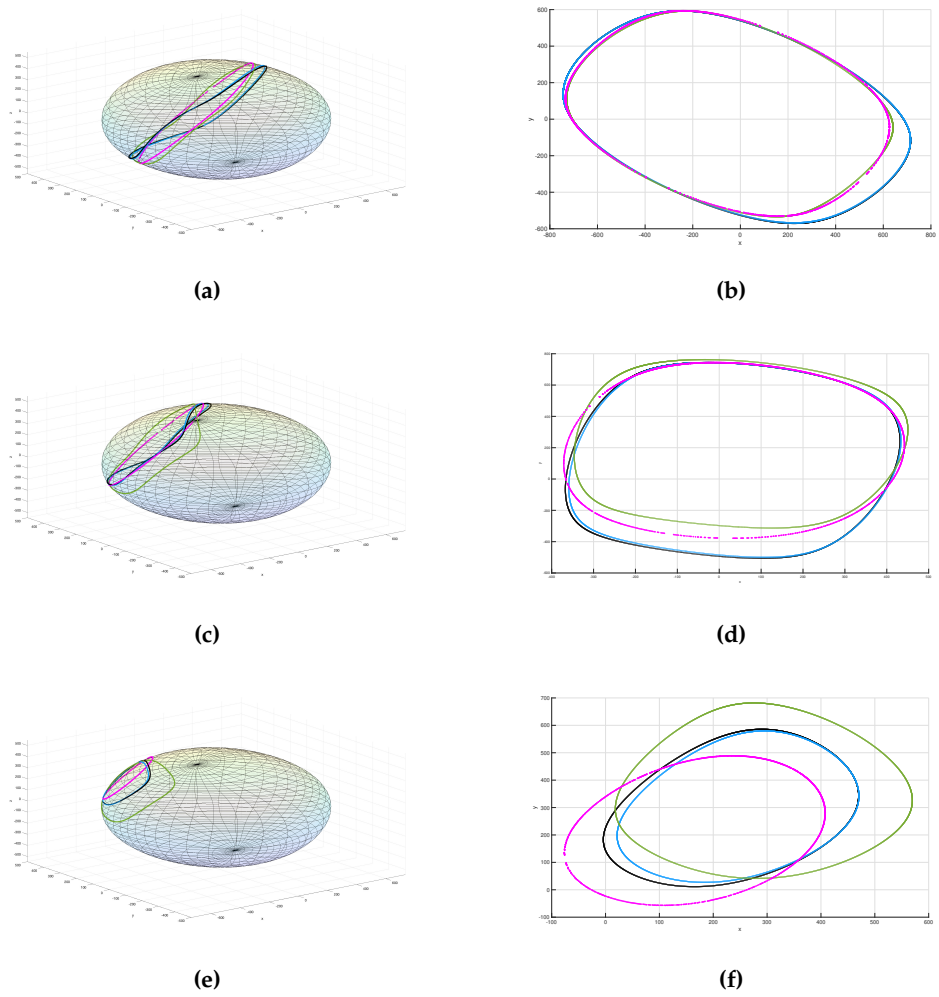


Figure 4. Parametric slices of Minkowski sum for a particular Minkowski sum and orientation of the slicing plane but at different heights h , computed by: MVOE from minimization of (7) (black), John's inner bound in (11) (blue), second eigenvalue $\lambda_2(A_i^T A_i)$ in (15a) (green). The actual slice of Minkowski sum is in pink.

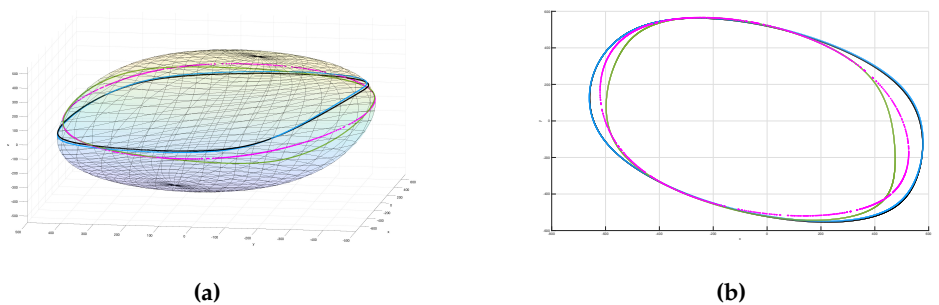


Figure 5. Parametric slices of Minkowski sum for similar Minkowski sum and height h of slicing plane to the sample in Figs. 4a, 4b, but for a different orientation of the plane, computed by MVOE from minimization of (7) (black), John's inner bound (11) (blue), second eigenvalue $\lambda_2(A_i^T A_i)$ in (15a) (green) and the actual slice of Minkowski sum (pink).

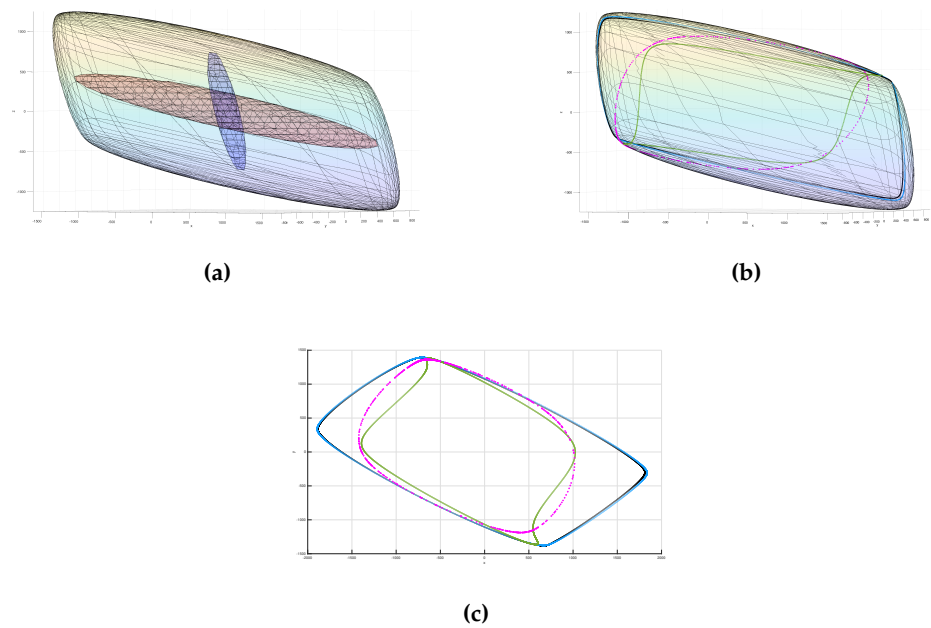


Figure 6. Parametric slices of Minkowski sum for a Minkowski sum of two ellipsoids with high aspect ratio of 8, sliced up by a similar plane to the sample in Figs.4a,4b. Here MVOE from minimization of (7) (black), John's inner bound (11) (blue), second eigenvalue $\lambda_2(A_i^T A_i)$ in (15a) (green) and the actual slice of Minkowski sum (pink).

is high between the major semi-axis and the second semi-axis, so that the ellipsoid has a "cigar" shape. For the same rationale of high curvature of the Minkowski surface, the parametric approximation of the slice of Minkowski sum of two cigar ellipsoids shows weak modeling of the actual slice.

4. Alternative Algorithm of a Narrow Strip for Slice of Minkowski Sum

In this section a computational algorithm is introduced to determine a "narrow strip" around the slice of Minkowski sum of ellipsoids, as an alternative approximation in the cases that the suggested parametric model of the slice returns a weak approximation. As discussed above, in regard to Figs.4e,4f, Fig.5 and Fig.6, these failure cases basically correspond to the slicing conditions in which the curve of the actual slice is closely passing through "corners" of the Minkowski surface with high curvatures.

The algorithm is demonstrated here in the case of slice of Minkowski sum of two ellipsoids in \mathbb{R}^3 . This strategy was basically inspired by the rationale behind (10), which indicates that the Minkowski sum of two ellipsoids, $E_1 \oplus E_2$, could be precisely constructed from intersection of countably infinite number of outer bounds from (7) or similarly from union of countably infinite number of inner bounds from (9). The idea here is to determine a "narrow strip" around the slice of Minkowski sum by using a few number of outer and inner ellipsoidal bounds of the Minkowski sum. In other words, it is expected that the elliptical slices of a few outer and inner ellipsoidal bounds of the Minkowski surface could be used to form a narrow strip around the slice of that Minkowski surface. Consider the Minkowski sum of two ellipsoids, which is sliced up far from the center of that Minkowski sum and close to its corner, as displayed in Fig.7a. A number of outer and inner bounds of the Minkowski are chosen and sliced up by the plane. In this example the elliptical slices of three ellipsoidal outer bounds are used to form an outer bound of the slice of Minkowski sum, namely the slices of the MVOE from minimization of (7) and two outer Kurzanski's bounds from (7) for $\beta = \lambda_{min}^{1/2}$ and $\beta = \lambda_{max}^{1/2}$, as shown in Figs.7a,7b. It is predictable from Fig.1 that in general the Kurzanski's outers for $\beta = \lambda_{min}^{1/2}$ and $\beta = \lambda_{max}^{1/2}$ touches a wider region of the boundary of Minkowski sum. Similarly, Figs.7a,7c show elliptical slices of

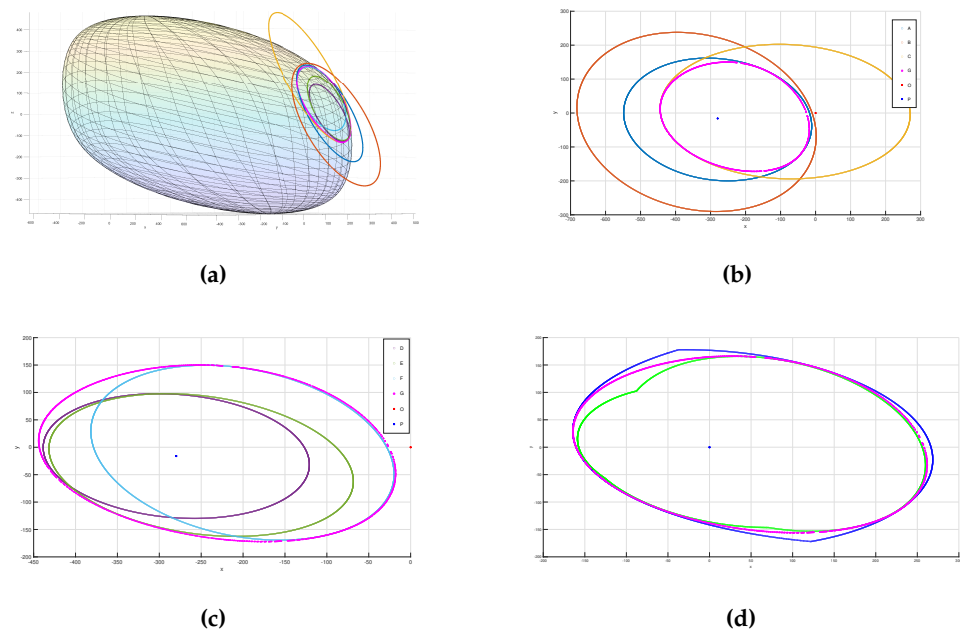


Figure 7. (a): slices of Minkowski sum, three outer and three inner bounds of Minkowski sum. (b) projection of slices of outer bounds in (a) onto the slicing plane, where bounds are by A: MVOE, B: outer Kurzanski's for $\beta = \lambda_{min}^{1/2}$, C: outer Kurzanski's for $\beta = \lambda_{max}^{1/2}$. (c) projection of slices of inner bounds in (a) onto the slicing plane, where bounds are by D: John's inner, E,F: inner Kurzanski's for two arbitrary $S_1, S_2 \in \mathbb{S}^+(n, \mathbb{R})$. Also G: projection of the actual slice of Minkowski sum, O: origin and P: an arbitrary point inside the actual slice. (d): Strip for slice of Minkowski sum (pink), obtained from slices of outer and inner bounds in (b) and (c).

three ellipsoidal inner bounds, namely the slices of the John's inner bound from (11) and two Kurzanski's inner bounds from (9) for two $S_1 \in \mathbb{S}^+(n, \mathbb{R})$, which are used to form the inner bound of the slice of Minkowski sum. It is notable from Figs.7b and 7c that the slices of MVOE and John's bound are not necessarily the minimum area outer ellipse and the maximum area inner ellipse, respectively among the elliptical slices of the all outer and inner Kurzanski's bounds. This is due to the fact that the size of the elliptical slices of the ellipsoidal bounds of the Minkowski sum depends not only on the size of the bounds but also on the orientation of the slicing plane. Then an arbitrary point, called the "new reference", is picked inside the slice of one of the inner bounds of the Minkowski sum. This new reference point is surely located inside the actual slice of Minkowski sum, since it is already inside the slice of one inner bound. The new reference point is shown in blue color in Fig.7 for differentiation from the original reference point in red. This new reference point inside the actual slice is then used to find one closest point to the actual slice (means also closest to the new reference point) among the three existing points on the three slices of outer bounds at every radial position within $\theta \in [0, 2\pi]$, measured from the new reference point. Similarly, applying this technique to three slices of three inner bounds the set of closest inner points to the actual slice (means farthest to the new reference point) is determined. As the result, the loci of closest points of the slices of outer and inner bounds to the actual slice form an outer bound (blue curve) and an inner bound (green curve) of the actual slice, which encloses it within a narrow strip as shown in Fig.7d. This algorithm is discussed in more details through several sub-algorithms A1 to A11 in appendix A.

This algorithm might be implemented for more number of outer and inner bounds of the Minkowski sum to increase the consistencies of the generated outer and inner bounds of the actual slice to the actual slice and consequently narrow the strip. For instance, more number of outer bounds could be used from the family of Kurzanski's outers in

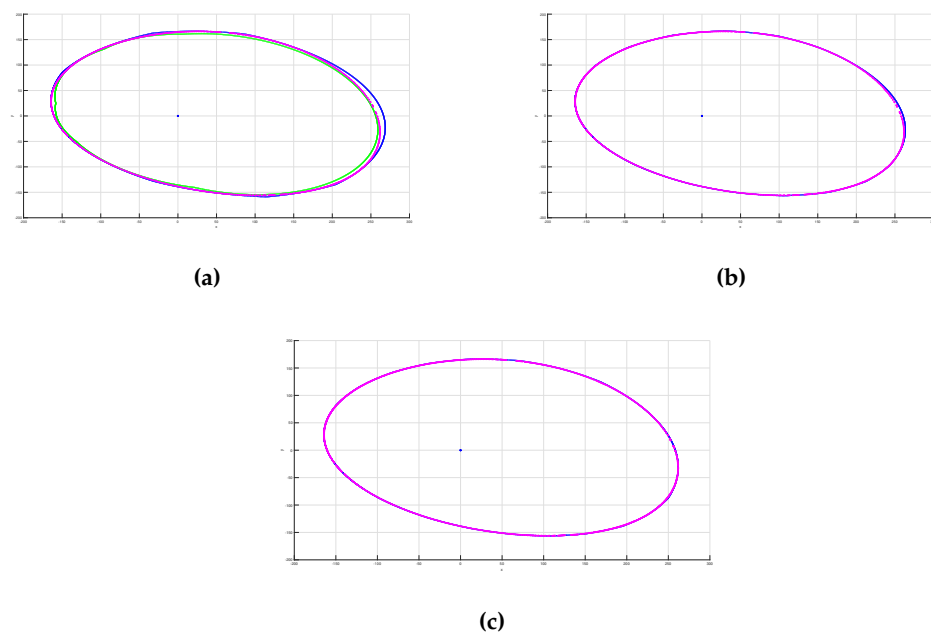


Figure 8. Strips for similar actual slice of Minkowski sum (pink) with Fig.7, obtained from (a): MVOE, four outer Kurzanski's, John's inner and four inner Kurzanski's, (b): MVOE and eight outer Kurzanski's, (c): MVOE and ten outer Kurzanski's.

(7), parametrized by $\beta \in [\lambda_{min}^{1/2}, \lambda_{max}^{1/2}]$ and similarly more number of inner bounds from the family of inner Kurzanski's in (9) for $\forall S \in \mathbb{S}^+(n, \mathbb{R})$. Fig.8a represents a narrower strip for the same actual slice in Fig.7, obtained by using MVOE, four outer Kurzanski's, John's inner and four inner Kurzanski's bounds. Figs.8b,8c approximate the same actual slice by successively MVOE and eight outer Kurzanski's and then MVOE and ten outer Kurzanski's, as both approximations precisely coincide on the actual slice. Note that these precise approximations are only constructed from more number of Kurzanski's outers, since as observed from comparison between Fig.1a and Fig.1b, it is predictable that in general an outer ellipsoidal bound touches a wider region of the boundary of Minkowski sum, compared to the touching region between an inner ellipsoid and the Minkowski sum boundary.

Figs.9a,9b and 9c successively show the strips generated by MVOE, four outer Kurzanski's, John's inner and four inner Kurzanski's for similar slicing samples in Fig.4e,4f, and Fig.5 and Fig.6, for which the suggested parametric model presented weak approximations of the actual slice.

5. Discussion

In this work a closed-form parametric equation was formulated, for the first time, to approximate the slice of Minkowski sum of finite number of ellipsoids in the case that the actual slice is relatively far enough from the corners of the Minkowski sum with high curvatures. Alternatively, an algorithm was suggested in the case that the actual slice passes closely through the corners of the Minkowski surface, in which a family of inner and outer bounds were used to construct a "narrow strip" for the slice of Minkowski sum. The algorithm was also applied in the case of slicing the Minkowski surface of ellipsoids with high aspect ratio. The results also approved that more number of outer and inner bounds of the Minkowski sum would increase the accuracies of the generated outer and inner bounds of the actual slice and consequently narrow the enclosing strip of the actual slice. In line with the goal, some ellipsoidal inner and outer bounds of the Minkowski sum were reviewed, including the so called "Kurzanski's" bounds. Also

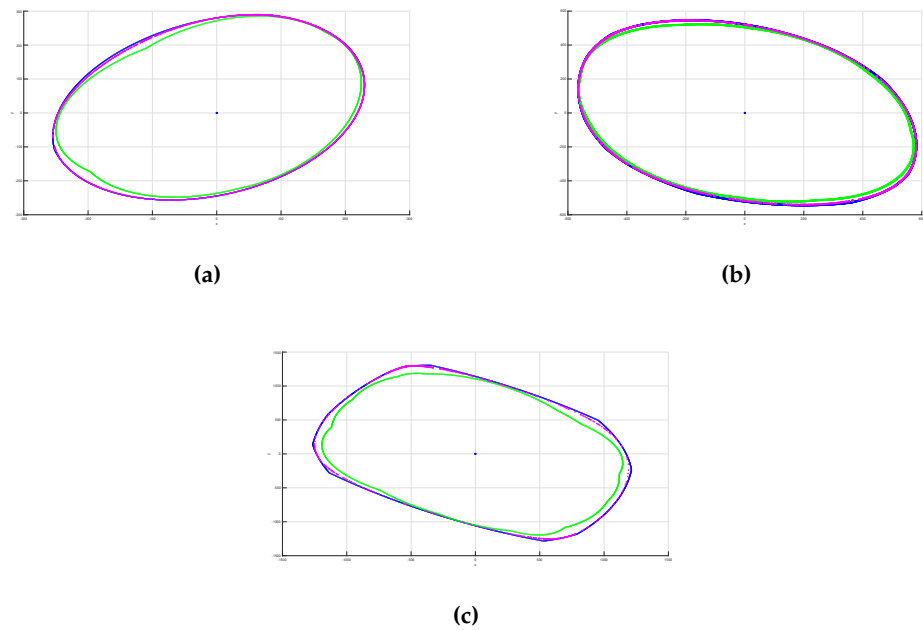


Figure 9. Strips generated by MVOE, four outer Kurzanski's, John's inner and four inner Kurzanski's for similar actual slices of Minkowski sums in (a): Fig.4e,4f, (b): Fig.5 and (c): Fig.6.

some ellipsoidal approximations of the Minkowski sum were suggested, which they do not necessarily bound the Minkowski sum from outside or inside, however they can be used, as well as the inner and outer bounds, in calculation of the developed parametric approximation of the slice of Minkowski sum. Precisely, the second eigenvalue-based parametric formula presented a more consistent approximation with the actual slice of Minkowski sum, compared to the outer-inner bound-based parametric formulas of the slice.

Appendix A. Algorithms:

Algorithm A1 Function: Slicing plane

Input: \mathbf{n} and h

Output: $\mathbf{u}_1, \mathbf{u}_2, \mathbf{p}_1, \mathbf{p}_2$

\mathbf{n} : Unit normal of plane

h : Height of plane.

$\mathbf{u}_1, \mathbf{u}_2$: Basis on the plane

$\mathbf{p}_1, \mathbf{p}_2$: Two points on the plane

Algorithm A2 Function: Domain of Kurzanski's outer bounds

Input: A_1, A_2

Output: $\lambda_{min}, \lambda_{max}$

$\{\lambda_1, \lambda_2, \lambda_3\} \leftarrow \text{Solve } \det(A_1^2 \lambda A_2^2) = 0$

$\lambda_{min} \leftarrow \min\{\lambda_1, \lambda_2, \lambda_3\}$

$\lambda_{max} \leftarrow \max\{\lambda_1, \lambda_2, \lambda_3\}$

Algorithm A3 Function: Compute a Kurzanski's outer bound

Input: $A_1, A_2, \lambda_{\min}, \lambda_{\max}$
 Output: A_β

Pick any $\beta \in [\lambda_{\min}^{1/2}, \lambda_{\max}^{1/2}]$

Use (7): $A_\beta \leftarrow [(1 + \beta^{-1})A_1^2 + (1 + \beta)A_2^2]^{1/2}$

Algorithm A4 Function: Compute a Kurzanski's inner bound

Input: A_1, A_2
 Output: $A_{[2]}$

Generate any $S_1 \in \mathbb{S}^+(3, \mathbb{R})$

Use (9):

$$A_{[2]} \leftarrow \left\{ S_1^{-1} \left[(S_1 A_1^2 S_1)^{1/2} + (S_1 A_2^2 S_1)^{1/2} \right]^2 S_1^{-1} \right\}^{1/2}$$

Algorithm A5 Function: Compute MVOE [24]

Input: $A_1, A_2, \epsilon_\beta, \lambda_{\min}, \lambda_{\max}$
 Output: β_{opt}, A_{MVOE}

Initial guess: $\beta_o \leftarrow \frac{\lambda_{\min}^{1/2} + \lambda_{\max}^{1/2}}{2} \in [\lambda_{\min}^{1/2}, \lambda_{\max}^{1/2}]$

$R_\beta \leftarrow A_1^{-1} A_2$

$\{\lambda_1, \lambda_2, \lambda_3\} \leftarrow \text{eig}(R_\beta)$

$\beta_{opt} \leftarrow \beta_o$

Error $\leftarrow \infty$

while Error $> \epsilon_\beta$ **do**

$N \leftarrow \sum_{i=1}^3 \frac{1}{1 + \beta_o \lambda_i}$

$D \leftarrow \sum_{i=1}^3 \frac{\lambda_i}{1 + \beta_o \lambda_i}$

$\beta_{opt} \leftarrow \left(\frac{N}{D} \right)^{1/2}$

Error $\leftarrow |\beta_{opt} - \beta_o|$

$\beta_o \leftarrow \beta_{opt}$

end while

$A_{MVOE} \leftarrow [(1 + \beta_{opt}^{-1})A_1^2 + (1 + \beta_{opt})A_2^2]^{1/2}$

Algorithm A6 Function: Compute the John's inner bound

Input: A_1, A_2
 Output: C_2

Use (11):

$$C_2 \leftarrow \left[A_1^2 + A_1 \left(A_1^{-1} A_2^2 A_1^{-1} \right)^{1/2} A_1 + \right. \\ \left. + A_2^2 + A_2 \left(A_2^{-1} A_1^2 A_2^{-1} \right)^{1/2} A_2 \right]^{1/2}$$

Algorithm A7 Function: Calculate elliptical slice of an ellipsoidal boundInput: $A, \mathbf{u}_1, \mathbf{u}_2, \mathbf{n}, h$ Output: $\mathbf{X}_{Slice3D}, \mathbf{X}_{Slice2D}$

$$h_s \leftarrow \frac{h}{\|A^T \mathbf{n}\|}$$

$$\mathbf{n}_s \leftarrow \frac{A^T \mathbf{n}}{\|A^T \mathbf{n}\|}$$

$$\mathbf{u}_s \leftarrow [-n_s^{(2)}, n_s^{(1)}, 0]^T$$

$$\mathbf{w}_s \leftarrow \frac{\mathbf{n}_s \times \mathbf{u}_s}{\|\mathbf{n}_s \times \mathbf{u}_s\|}$$

$$r_s \leftarrow \sqrt{1 - h_s^2}$$

$$C_s \leftarrow [\mathbf{u}_s \quad \mathbf{w}_s] \begin{bmatrix} r_s & 0 \\ 0 & r_s \end{bmatrix}$$

$$\mathbf{X}_{Slice3D} \leftarrow h_s A \mathbf{n}_s + A C_s \mathbf{u} \quad \text{where: } \mathbf{u} \in \mathbb{S}^2$$

$$X_{Slice2D}^{(1)} \leftarrow X_{Slice3D} \cdot \mathbf{u}_1$$

$$X_{Slice2D}^{(2)} \leftarrow X_{Slice3D} \cdot \mathbf{u}_2$$

$$\mathbf{X}_{Slice2D} \leftarrow [X_{Slice2D}^{(1)}, X_{Slice2D}^{(2)}]^T$$

Algorithm A8 Function: Choose a new origin inside actual slide of Minkowski sumInput: $X_{Slice2D}$ Output: \mathbf{O}_{new}

$$O_{new}^{(1)} \leftarrow \frac{\sum X_{Slice2D}^{(1)}}{m} \quad \text{where: } m \text{ is number of points in } X_{Slice2D}$$

$$O_{new}^{(2)} \leftarrow \frac{\sum X_{Slice2D}^{(2)}}{m}$$

$$\mathbf{O}_{new} \leftarrow [O_{new}^{(1)}, O_{new}^{(2)}]^T$$

Algorithm A9 Function: Switch the origin to the new oneInput: $\mathbf{O}_{new}, \mathbf{X}_{Slice2D}, m$ Output: $\mathbf{X}_{SortNewSlice2D}$

$$\mathbf{X}_{NewSlice2D} \leftarrow \mathbf{X}_{Slice2D} - \mathbf{O}_{new}$$

$$\mathbf{X}_{SortNewSlice2D} \leftarrow \text{Sort}(\mathbf{X}_{NewSlice2D}) \text{ by angle measured from new origin for each point}$$

Algorithm A10 Function: Outer layer of strip of slice of Minkowski sumInput: $\mathbf{X}_{SortOuterSlice2D}^{(j)}$ for $j \in \{1, 2, \dots, k\}$ number of Kurzhanski's outer boundsOutput: $OuterStrip$ **for** $i = 1 \rightarrow m$ **do****for** $j = 1 \rightarrow k$ **do**

$$Norm(i, j) \leftarrow \|\mathbf{X}_{SortOuterSlice2D}^{(i,j)}\| \text{ of point } i \text{ of outer bound } j$$

end for

$$OuterStrip(i) \leftarrow \min_{j \in \{1, 2, \dots, k\}} \{Norm(i, j)\}$$

end for

Algorithm A11 Function: Inner layer of strip of slice of Minkowski sum

Input: $\mathbf{X}_{\text{SortInnerSlice2D}}^{(j)}$ for $j \in \{1, 2, \dots, k\}$ number of Kurzshanski's inner bounds
 Output: *InnerStrip*

```

for  $i = 1 \rightarrow m$  do
  for  $j = 1 \rightarrow k$  do
     $\text{Norm}(i, j) \leftarrow \|\mathbf{X}_{\text{SortInnerSlice2D}}^{(i,j)}\|$  of point  $i$  of inner bound  $j$ 
  end for
   $\text{InnerStrip}(i) \leftarrow \max_{j \in \{1, 2, \dots, k\}} \{\text{Norm}(i, j)\}$ 
end for

```

References

- Shiffman, B.; Lyu, S.; Chirikjian, G.S. Mathematical aspects of molecular replacement. V. Isolating feasible regions in motion spaces. *Acta Crystallographica Section A* **2020**, *76*, 145–162. <https://doi.org/10.1107/S2053273319014797>.
- Shiffman, B.; Chirikjian, G. Collision-free configuration-spaces in macromolecular crystals. *Robotica* **2016**, *34*, 1679–1704.
- Ruan, S.; Poblete, K.L.; Wu, H.; Ma, Q.; Chirikjian, G.S. Efficient Path Planning in Narrow Passages for Robots With Ellipsoidal Components. *IEEE Transactions on Robotics* **2022**.
- Latombe, J.C. *Robot Motion Planning*, 1 ed.; Springer US, 1991.
- E.E, H.; J.P, M.; K., S.; H.B, V.; J, Z. A computing strategy for applications involving offsets, sweeps, and Minkowski operations. *Computer aided design* **1999**, *31*, 175–183.
- Halperin, D.; Latombe, J.C.; Wilson, R.H. A General Framework for Assembly Planning: The Motion Space Approach. *Algorithmica* **2000**, *26*, 577–601.
- Yan, Y.; Chirikjian, G.S. Closed-form characterization of the Minkowski sum and difference of two ellipsoids. *Geometriae Dedicata* **2015**, *177*, 103–128.
- Chirikjian, G.S. *Harmonic Analysis for Engineers and Applied Scientists: Updated and Expanded Edition*; Dover, 2016.
- Dummit, D.S.; Foote, R.M. *Abstract Algebra*, 3rd ed.; Wiley, 2003.
- Hungerford, T.W. *Algebra*, 8th ed.; Springer, 1980.
- Chirikjian, G.S.; Shiffman, B. Applications of convex geometry to Minkowski sums of m ellipsoids in \mathbb{R}^n : Closed-form parametric equations and volume bounds. *International Journal of Mathematics* **2021**, *32*, 2140009, <https://doi.org/10.1142/S0129167X21400097>.
- Ruan, S.; Chirikjian, G.S. Closed-form Minkowski sums of convex bodies with smooth positively curved boundaries. *Computer-Aided Design* **2022**, *143*, 103133.
- Alfano, S.; Greer, M.L. Determining If Two Solid Ellipsoids Intersect. *Journal of Guidance, Control, and Dynamics* **2003**, *26*, 206–210.
- Goodey, P.; Weil, W. Intersection bodies and ellipsoids. *Mathematika* **1995**, *42*, 295–304.
- Perram, J.W.; M.S.Wertheim. Statistical mechanics of hard ellipsoids. I. Overlap algorithm and the contact function. *Journal of Computational Physics* **1985**, *58*, 409–416.
- Kurzshanski, A.; Valyi, I. *Ellipsoidal Calculus for Estimation and Control*, 1 ed.; Systems and control : foundations and applications, Birkhäuser Basel, 1997.
- Kurzshanskiy, A.A.; Varaiya, P. Ellipsoidal Toolbox (ET). *Proceedings of the 45th IEEE Conference on Decision and Control* **2006**, pp. 1498–1503.
- Ros, L.; Sabater, A.; Thomas, F. An ellipsoidal calculus based on propagation and fusion. *IEEE Transactions on Systems, Man, and Cybernetics, Part B (Cybernetics)* **2002**, *32*, 430–442.
- Durieu, C.; Walter, É.; Polyak, B.T. Multi-Input Multi-Output Ellipsoidal State Bounding. *Journal of Optimization Theory and Applications* **2001**, *111*, 273–303.
- Sholokhov, O.V. Minimum-volume ellipsoidal approximation of the sum of two ellipsoids. *Cybernetics and Systems Analysis*, **2011**, *47*, 954–960.
- Kurzshanski, A.; Varaiya, P. Reachability analysis for uncertain systems-The ellipsoidal technique. *Dynamics of Continuous, Discrete and Impulsive Systems. Series B: Applications and Algorithms* **2002**, *9*.
- Schweppe, F. *Uncertain Dynamic Systems*; Prentice-Hall, 1973.
- MAKSAROV, D.; NORTON, J.P. State bounding with ellipsoidal set description of the uncertainty. *International Journal of Control* **1996**, *65*, 847–866.
- Halder, A. On the Parameterized Computation of Minimum Volume Outer Ellipsoid of Minkowski Sum of Ellipsoids. *IEEE Conference on Decision and Control (CDC)* **2018**, *1*, 4040–4045.
- Busemann, H. The foundations of Minkowskian geometry. *Commentarii Mathematici Helvetici volume* **1950**, *24*, 156–187.
- John, F. Extremum Problems with Inequalities as Subsidiary Conditions. *Traces and Emergence of Nonlinear Programming* **2014**, pp. 197–215.

27. Chernousko, F.L. *State Estimation for Dynamic Systems*, 1st ed.; CRC Press, 1993.